JGR Biogeosciences

RESEARCH ARTICLE
10.1029/2018JG004573

Tree Ring Reconstructions of Stemwood Biomass Indicate Increases in the Growth Rate of Black Spruce Trees Across Boreal Forests of Canada

Robbie A. Hember[1], Werner A. Kurz[2], and Martin P. Girardin[3]

[1]Climate Change and Integrated Planning, BC Ministry of Forests, Lands, Natural Resource Operations and Rural Development, Victoria, British Columbia, Canada, [2]Pacific Forestry Centre, Canadian Forest Service, Natural Resources Canada, Victoria, British Columbia, Canada, [3]Laurentian Forestry Centre, Canadian Forest Service, Natural Resources Canada, Sainte-Foy, Quebec, Canada

Key Points:
- Tree ring observations indicate that growth of black spruce trees increased between 1901 and 2001 over boreal forests of Canada
- Samples represent trees that were live and dominant at time of sampling, which confounds the attribution of trend to environmental change
- Adjusting trends in growth to account for natural dynamics suggested that environmental changes collectively drove an increase in growth of 47–82%

Supporting Information:
- Supporting Information S1

Correspondence to:
R. A. Hember,
robert.hember@gov.bc.ca

Citation:
Hember, R. A., Kurz, W. A., & Girardin, M. P. (2019). Tree ring reconstructions of stemwood biomass indicate increases in the growth rate of black spruce trees across boreal forests of Canada. *Journal of Geophysical Research: Biogeosciences*, *124*, 2460–2480. https://doi.org/10.1029/2018JG004573

Received 10 MAY 2018
Accepted 11 JUL 2019
Accepted article online 16 JUL 2019
Published online 6 AUG 2019

Abstract The claim that changes in atmospheric composition and climate have enhanced the growth rate of trees is prevalent in science, yet it is not supported by many recent tree ring studies. In this study, we analyzed historical time trends in stemwood biomass growth derived from black spruce (*Picea mariana* (Mill.) BSP) trees at 248 plots across Canada. The sample consisted of trees that were live and dominant at the time of sampling (LDS). Observations of stemwood biomass of LDS trees at a reference age of 75 years ($B_{sw75,LDS}$) increased by 154 to 321% over 1901–2001 depending on the method of trend estimation. Simulations from a calibrated individual-based Growth and Yield model—forced with varying degrees of hypothetical trend in tree growth—were used to estimate the proportion of trend that could be attributed to intrinsic factors, including artefacts introduced by sampling from LDS trees instead of from the population of trees. Imposing no time trend in simulated tree growth, stemwood biomass of 75-year-old LDS trees ($B_{sw75,LDS,Model}$) increased by 63% (41 to 85% CI). We conclude that the remaining variation in growth of LDS trees (154 to 321% minus 63% = 91 to 258%) can be attributed to net extrinsic forcing. The scaling relationship between LDS and population trees further suggested that stemwood biomass growth of the population ($G_{sw75,POP}$) increased by 47 to 82%. By accounting for both natural dynamics and artefacts of the sampling design in estimation of net intrinsic forcing, we gained confidence that growth rate of black spruce trees across Canada increased significantly over 1901–2001. While growth enhancement is consistent with beneficial effects of increasing levels of reactive nitrogen, carbon dioxide, and warming, there remains uncertainty in the degree that applied procedures fully account for known sampling artefacts.

1. Introduction

There is a common assumption in global carbon cycle science that changes in atmospheric composition and climate have increased the growth rate of trees (Ciais et al., 2013; King et al., 2007; Prentice et al., 2001). Increases in atmospheric concentrations of reactive nitrogen (~1 to 20 kg N ha^{-1} yr^{-1}) and carbon dioxide concentration (~120 ppm), in addition to warming (~0.6 to 1.2 °C), should partially alleviate constraints imposed by suboptimal supplies of nitrogen, carbon, and heat, respectively. The claim is most commonly supported by simulations using biochemical models of photosynthesis (Arora et al., 2013; Cao & Woodward, 1998; Chen et al., 2000; Cramer et al., 2001; Friedlingstein et al., 2006; Mackenzie et al., 2002; Piao et al., 2013; Sitch et al., 2008). However, it is also supported by the average response of trees to increased nitrogen supply (LeBauer & Treseder, 2008; Xia & Wan, 2008), enriched carbon dioxide concentration (Idso & Idso, 1994; Kirschbaum & Lambie, 2015; Norby et al., 1999; Saxe et al., 1998; Wullschleger et al., 1995), and warming (Way & Oren, 2010). Studies of stand-level biomass dynamics in humid boreal and temperate forests also consistently suggest that natural dynamics, such as change in stand age, cannot fully explain positive time trends in aboveground biomass production, implying a significant positive effect of environmental changes on tree growth (Erb et al., 2013; Fang et al., 2014; Hember et al., 2012; Hember et al., 2017a; Kauppi et al., 2014; Pan et al., 2011; Pretzsch et al., 2014).

Some studies of individual-tree growth report positive trends that implicate environmental change (Cole et al., 2009; Kint et al., 2012; Voelker et al., 2006), yet other studies have cautioned that a proportion of time trends in growth may be related to artefacts of the sampling design (Bowman et al., 2013; Brienen et al., 2012; Duchesne et al., 2019; Nehrbass-Ahles et al., 2014). Numerous other studies with extensive sampling and

broad geographic coverage report an absence of time trends (Gedalof & Berg, 2010; Girardin et al., 2016; Peñuelas et al., 2011) or decreasing trends in growth (Barber et al., 2000; Dietrich et al., 2016; Hogg et al., 2017; Silva et al., 2010).

Varying evidence of time trends in primary productivity, including tree ring-based studies of tree growth, must partially reflect differences in region, species, and time period of analysis. Among studies of stand-level net biomass production, there is a distinction between evidence of positive time trends in wet boreal and temperate forest regions (Hember et al., 2012; Hember, Kurz, & Coops, 2017a; Kauppi et al., 2014; McMahon et al., 2010; Pan et al., 2011; Pretzsch et al., 2014) and negative time trends in dry boreal regions (Chen & Luo, 2015; Hember, Kurz, & Coops, 2017a). There is no discrepancy among those studies if one assumes that beneficial effects of environmental change are confined to wetter climates. Although this pattern is upheld by stand-level studies, it breaks down among tree ring-based studies, where positive time trends are frequently absent regardless of hydrological conditions (Barber et al., 2000; Bond-Lamberty et al., 2014; Dietrich et al., 2016; Gedalof & Berg, 2010; Girardin et al., 2016, 2015; Silva et al., 2010). Yet in tree ring studies, there are also substantial differences among analytical methods and differences in how extensively studies attempt to disentangle intrinsic and extrinsic controls on temporal variability of growth.

Most tree-level studies assess tree growth by coring and analyzing the annual rings of stemwood. In general, a subset of trees within a site is cored and rings are cross-dated to form site samples. Multiple site chronologies are combined to form regional samples. Studies analyze ring width (w), basal area increment (BAI), or stemwood biomass growth (G_{sw}).

Standardization, also known as "detrending," is used to distinguish a specific effect of interest (e.g., time or temperature) from all the other effects contributing to total variation in tree growth (Becker, 1989; Bontemps & Esper, 2011; Briffa & Melvin, 2011; Peters et al., 2015; Schofield et al., 2016). Some studies take a minimalist approach to data manipulation and do not standardize observations (Beck et al., 2011; Jump et al., 2006; Salzer et al., 2009; Silva et al., 2010). Studies commonly apply "traditional" standardization (Schofield et al., 2016), where age-response functions are fitted to observations, then used to remove the variance explained by age, before inferring the effect of interest from the residuals or response ratios. Within traditional standardization, one can distinguish whether fitting is performed on individual trees, or all sampled trees within each site. Acknowledging that tree- or site-level standardization might not accurately reflect the marginal response of growth to intrinsic factors, such as age, studies introduced "regional curve" standardization, fitting the age response to pooled sites (Becker, 1989; Dietrich et al., 2016; Esper et al., 2003). It marked acknowledgement that the correlation among tree age, tree size, and time for individual trees, or within individual sites, is usually strong, and that the ability to differentiate between intrinsic and extrinsic sources of temporal variation in field observations hinges on sampling from a large, evenly mixed multivariate response space. In tree ring studies, this effectively means pooling sites across a wide range of establishment dates.

Statistical modeling has been applied to pooled tree ring data and differs from regional curve standardization only by considering predictor variables simultaneously based on conventional methods of estimation, such as least squares (LS) multiple regression or mixed-effect (ME) modeling (Cole et al., 2009; Kint et al., 2012; Martin-Benito et al., 2011; Schofield et al., 2016). Due to the longitudinal nature of tree ring samples, application of ME models has become common (Fajardo & McIntire, 2012; Girardin et al., 2016; Martin-Benito et al., 2011). Within the statistical modeling approach, there are studies that express extrinsic factors indirectly by testing whether time is a significant covariate, while other studies test whether environmental variables are significant covariates. Another distinguishing feature of such studies is whether intrinsic effects are represented by age, or age and other factors, such as size of the tree, or the competitive status of the tree.

Fewer studies infer tree growth indirectly from the age response of tree size (Bascietto et al., 2004; Hember et al., 2012; McMahon et al., 2010; Mund et al., 2002; Pretzsch et al., 2014; Spiecker, 1999), including outside-bark diameter (D_{ob}), basal area (BA), or stemwood biomass (B_{sw}). This can be achieved by selecting a reference age, A_{ref}, and testing for time dependence in size at a reference age, B_{sw} (A_{ref}). This approach inherently avoids the need to account for size dependence in multiple regression models of growth directly, which poses a problem because collinearity between tree size and time will weaken the performance of multiple

regression analysis. Although this approach can indicate whether mean growth has changed, it falls short of resolving interannual variability.

Lastly, studies vary by whether they acknowledge sampling artefacts as a potential contributor to time trends. For example, it has been shown that tendencies to exclude small trees, as well as the exclusion of trees that died prior to the sampling date, can influence the variation of survivor growth leading up to the sampling date (Brienen et al., 2012; Briffa & Melvin, 2011; Nehrbass-Ahles et al., 2014). Across landscapes, it has also been proposed that relationships between stand productivity and probability of harvest can lead to a disproportionate number of productive stands in younger age classes (Krankina et al., 2005). This could also translate into artefacts at the tree level, influencing variation of survivor growth (pooled across sampling sites) with time before sampling. If the most productive stands are subjected to higher probability of disturbance, then they may be increasingly underrepresented in tree ring samples with increasing time before sampling.

To understand whether time trends in growth rate of black spruce (*Picea mariana* (Mill.) BSP) trees exist across Canada, we attempted to maneuver through these postprocessing complexities using a large sample of tree ring chronologies from Canada's National Forest Inventory (NFI). The study expanded on previous analysis of time trends in black spruce trees across Canada (Girardin et al., 2016) by considering a different methodology and extending the analysis back to 1901. The objectives of the study were threefold. First, we presented a rationale for key decisions that must be made during postprocessing of tree ring samples. Second, we estimated the time trend in stemwood biomass of cored trees using three common methods. Third, we referred to simulations from a Growth and Yield model to better understand the proportion of time trend that can be explained by intrinsic factors.

2. Data

See Table 1 for a list of variables used in the study.

2.1. Tree Ring Data

The tree cores were collected and processed as part of Canada's National Forest Inventory and tree ring data were compiled and reassessed for quality control. The study included all field plots containing cores of black spruce within the Boreal Cordillera, Boreal Plain, and Boreal Shield ecozones (Figure 1). NFI documentation indicated that measurements of ring width, w, were multiplied by a factor of 1.1 to account for shrinkage

Table 1
List of Variables

Symbol	Units	Description
A	year	Tree age
A_{ref}	year	A reference level of tree age at which variation in size is analyzed and reported
BA	cm^2	Basal area of tree stemwood
BAI	cm^2/year	Annual tree basal area increment
B_{sw}	kg C	Stemwood biomass
D_{ib}	cm	Diameter at breast height, inside bark
D_{ob}	cm	Diameter at breast height, outside bark
D	-	Denoting trees that were dominant
G_{sw}	kg C/year	Stemwood biomass growth rate
LDS	-	Denoting trees that were live and dominant at the time of sampling
LS	-	Denoting trees that were live at the time of sampling
POP	-	Denoting trees that were from the stand population
SB	Mg C/ha	Stand biomass density
SBLT	Mg C/ha	The amount of biomass in trees that are larger than the focal tree
SD	trees/ha	Stand density (tree population density)
t	year	Time
t_{samp}	year	Time of sampling
T	°C	Mean warm-season (May–September) air temperature, 1971–2000
w	mm/year	Ring width or annual radial increment
W	mm	Mean warm-season (May–September) soil water content, 1971–2000

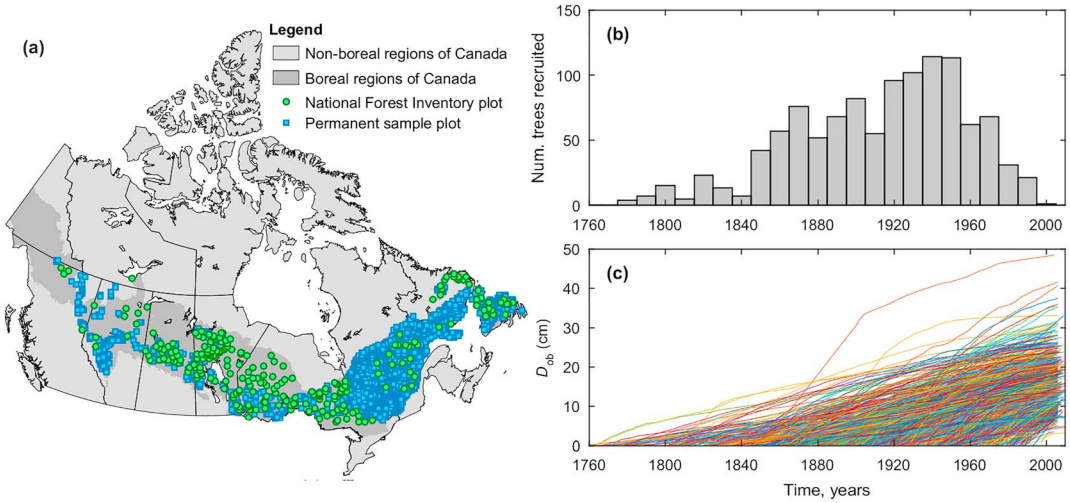

Figure 1. Measurements of black spruce across boreal ecozones of Canada. (a) Map of National Forest Inventory plots with cored black spruce trees and permanent sample plots used in Growth and Yield model calibration. (b) Number of recruited trees in the tree ring sample. (c) Time series of outside-bark diameter of cored trees (D_{ob}).

during drying of the cores. The cumulative annual ring width values were used to reconstruct the chronology of outside-bark diameter (D_{ob}) for each core, assuming that bark thickness was equal to 6% of inside-bark stemwood diameter (Li & Weiskittel, 2011). The database also included tape-based measurements of D_{ob} at the time of sampling (t_{samp}). Cores that failed to intersect the pith were adjusted based on a distance-to-pith correction, which was estimated using a digital concentric ring tool when the number of missing rings was small (i.e., when the curvature was identified), or estimated using the difference between tape- and core-based estimates of D_{ob} when the number of missing rings was large (Hogg et al., 2017). Cores were then cross-dated using the COFECHA program (Holms, 1983). Pooling the tree ring data indicated relatively strong agreement ($R^2 = 0.90$) between core- and tape-based estimates of D_{ob} at the time of sampling (not shown). Core-based estimates of D_{ob} were systematically smaller than tape-based estimates of D_{ob} by 0.5 $\pm$ 0.2 cm. Residuals were not correlated with age ($p = 0.56$) or with D_{ob} ($p = 0.41$). Core-based reconstructions of D_{ob} were converted to stemwood biomass (B_{sw}) using allometric equations for black spruce (Lambert et al., 2005) and then converted to units of carbon assuming a carbon-dry weight ratio of 0.5 (Lamlom & Savidge, 2003). The age responses of core-based reconstructions of tree size and annual growth rate were inspected on a plot-by-plot basis for quality assurance.

2.2. Environmental Data

Warm-season (May–September) air temperature was calculated from ClimateNA (Wang et al., 2006). Warm-season soil water content was calculated from a monthly surface water balance model (Hember et al., 2017b; Hember, Kurz, & Coops, 2017a). The model followed previous implementations of Thornthwaite's initial approach (Willmott et al., 1985), only replacing the temperature-based model of actual evapotranspiration with the Penman-Monteith equation for forest canopies with moderate atmosphere-canopy coupling (Hember, Coops, & Spittlehouse, 2017). Values for each tree were derived from the nearest cell within a 1-km grid. As the climate variables represented averages from the 1971–2000 base period, values were constant over the time series of each tree.

2.3. Summary of Sample Properties

The final tree ring sample consisted of 98,068 measurements of annual tree growth, from 2,062 individual trees, distributed across 248 plots. According to site classification of each plot, 172 (69%) were classified as upland forest sites, while the remaining 76 (31%) were classified as peatland sites. Time of tree recruitment ranged from 1774 to 1983 with a mean of 1892 (Figure 1b and Table S1).

The boreal forest ecozones of Canada covered all classes from Thornthwaite's climate classification system, ranging from hyperhumid to arid. As tree growth is associated with hydrological conditions (Girardin et al., 2015; Hember, Kurz, & Coops, 2017a; Hogg et al., 2017; Sullivan et al., 2017), documenting the hydrological

conditions of the sample may help to understand differences among studies. Here approximately 45% of the study area was classified as subhumid, semiarid, or arid (herein designated collectively as "dry"). Of the area where black spruce was present in spatialized inventories (Beaudoin et al., 2014), approximately 43% was classified as dry. Weighting that estimate by the estimated abundance of black spruce, just 35% of the distribution of black spruce was classified as dry. Of the NFI sample with cored black spruce, just 31% was classified as dry. As such, hydrological conditions of the core sample were approximately representative of the species distribution.

The core sample consisted of trees from all parts of the tree size distribution of each plot, but samples were mostly obtained from dominant trees. The dominance of the core sample was assessed by calculating the percentile of D_{ob} from all trees in the plot census that corresponded with the mean value of D_{ob} of cored trees for each plot, and then pooling the percentile from each plot to calculate a mean percentile of the 248 plots. This pooled mean indicated that the core sample of black spruce trees, on average, represented the 89th percentile of tree size within plots.

2.4. Growth and Yield Model

Simulations were performed using an individual-based Growth and Yield model, *Sawtooth* (Hember & Kurz, 2018). The model was calibrated against periodic observations of black spruce trees at permanent sample plots (PSPs) maintained by agencies in British Columbia, Alberta, Saskatchewan, Manitoba, Ontario, Québec, and Newfoundland and Labrador (Figure 1a). The model predicted stand-level biomass dynamics based on species-specific equations of recruitment, mortality, and growth rate of individual trees. The annual probability of recruitment was predicted as a function of stand biomass density (SB). The annual probability of mortality was predicted as a function of stand age, SB, biomass of larger trees (SBLT), and nonlinear dependence on biomass of the focal tree. The inclusion of SB and SBLT were meant to express actual and relative intensities of competition. Likewise, annual growth rate of live trees was predicted based on stand age, SBLT, SB, and nonlinear dependence on biomass of the focal tree. During preliminary analysis, we compared simulations and observed stemwood biomass dynamics at the level of stands (Figure S1) and at the level of individual trees (Figures S2 and S3).

3. Methods

3.1. Analytical Framework

Actual temporal variation in growth is controlled by numerous explanatory factors, and the impact of those individual explanatory factors can be characterized by the temporal forcing they impose on growth (Hember, Kurz, & Coops, 2017a). The temporal forcing imposed on growth by an explanatory factor is defined by the sensitivity of growth to that explanatory factor, multiplied by the magnitude of change in that explanatory factor over time. As tree growth is linked to both natural dynamics and environmental change, it is conceptually and quantitatively helpful to differentiate between these sources of variation by categorizing them into intrinsic or extrinsic forcings, respectively.

The objective of this study is to estimate the net extrinsic forcing of growth, which expresses the net forcing from all changes in environmental conditions over time. As growth is sensitive to numerous intrinsic and extrinsic factors that vary over time, net extrinsic forcing is unlikely to equal actual temporal variation in tree growth. As intrinsic and extrinsic factors are typically correlated, both varying with time, the omission of any primary intrinsic or extrinsic factors may constitute underspecification of the analytical framework, with potentially adverse effects on the accuracy of trend attribution. Among studies that discuss potential sources of error in the estimation of time trends in tree ring data, "bias" has been used most commonly to describe false attribution of temporal variation in growth to extrinsic factors. Yet here we argue that false attribution of temporal variation in growth to intrinsic factors warrants equal consideration.

3.2. Summary of Analytical Steps and Rationale

Prior to description of methods, we outline the key decisions and potential sources of bias that are relevant to estimation of time trends in tree growth using tree ring data (Figure 2). The first choice one faces is whether to analyze time trend in the growth or size of trees (Decision 1). Most studies focus on growth, but some also analyze size. If the decision is made to analyze growth, the second choice is whether to analyze ring width, basal area increment, or stemwood biomass growth (Decision 2). Studies of width or basal area increment

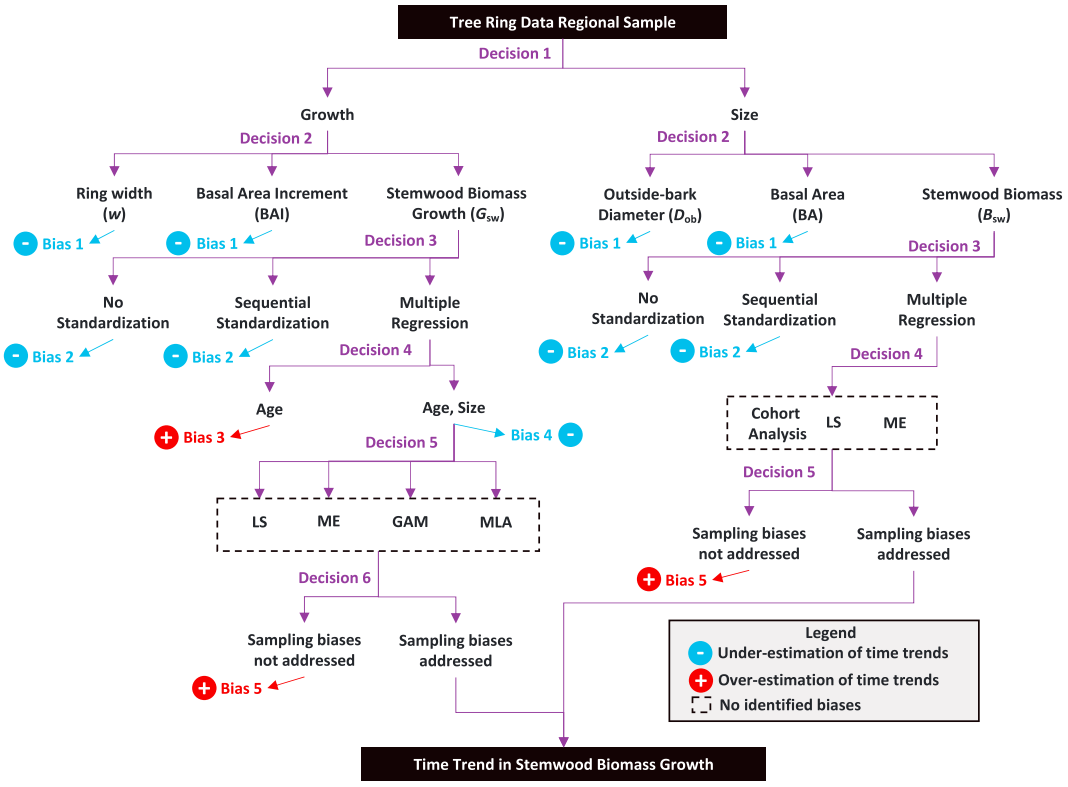

Figure 2. Summary of options to analyze time trends in tree ring data, including key decisions and preliminary identification of potential sources of bias. Positive bias indicates an argument that the decision in question may lead to overestimation of time trend, be it positive or negative, while negative bias indicates an argument that the decision in question may lead to underestimation of time trend. LS regression, ME modeling, generalized additive modeling, machine learning algorithms.

must acknowledge that, even in a relative scale, results are not directly comparable with stemwood biomass growth (Hember et al., 2015; Hunter & Schuck, 2002). When the objective is strictly to estimate the time trend in stemwood biomass growth, analysis of ring width is expected to introduce negative bias (i.e., underestimation of time trends) because it only constitutes one dimension of a three-dimensional system (Bias 1). If carbohydrates were hypothetically allocated to cambial and apical growth in a 2:1 ratio (i.e., equal growth in length, width, and height), a +100% stimulus in G_{sw} ought to yield a 26% increase in w, as it constitutes the elongation of just one dimension. Many studies focus on BAI, stating that it is more closely related to G_{sw}. Analyzing BAI circumvents the component of variation in w that is attributed to geometry of the tree (i.e., decreasing ring width with increasing tree radius) and it diminishes the expected magnitude of Bias 1, as a +100% stimulus in G_{sw} should translate into a 59% increase in BAI. The last option is to reconstruct D_{ob} and then convert it to B_{sw} using allometric equations, and finally calculating G_{sw} from the annual difference in B_{sw}. The use of allometric equations introduces uncertainty because tree height is most often unknown, such that one must rely on diameter-only allometric equations. However, there is no strong a priori reason to expect the relationships between G_{sw} and D_{ob} to introduce a systematic error in time trend.

Studies must then choose how to estimate the effect of various known intrinsic and extrinsic factors on growth (Decision 3). As expected for a "classic" tree ring sampling design (Nehrbass-Ahles et al., 2014), G_{sw} in the present sample was correlated with size, age, and time (Table S2). Age is an intrinsic factor and the average age of the sample tends to increase with time. It is commonly assumed that growth is negatively correlated with age following canopy closure, as supported by the negative partial correlation found here (Table S2). We, therefore, propose that applying no standardization to account for intrinsic forcing (associated with aging of the sample over time) risks misinterpreting the actual observed variability in growth as extrinsic forcing.

Sequential standardization is defined as any approach that estimates the sensitivity to extrinsic factors from a sequence in procedure, first estimating and removing variation explained by intrinsic factors (e.g., age and/or tree size) and second estimating the variance explained by time in what variation remains in the residuals from the first step. Variants of sequential standardization include those that apply standardization at the scale of individual trees, sites, and regions. Sequential standardization does not objectively test the ability of both intrinsic and extrinsic factors to decrease the sum of squared error in growth (Darlington & Smulders, 2001; Freckleton, 2002; García-Berthou, 2001). As intrinsic and extrinsic factors are consistently correlated in the classic sampling design, we anticipate that sequential standardization risks underestimating time trends in growth (Bias 2).

Multiple regression analysis was defined here as any approach that estimates the sensitivity to all intrinsic and extrinsic factors simultaneously using a statistical model. Although multiple regression is not immune to error in estimation of correlated effects, it avoids the subjectivity associated with estimating the sensitivity to intrinsic and extrinsic factors in sequence.

Studies that apply multiple regression analysis of growth must choose whether to include or exclude tree size as an intrinsic factor (Decision 4). The dependence of growth rate on tree size is difficult to estimate. Growth of perennials is correlated with body size (Paine et al., 2012; Sheil et al., 2017; Stephenson et al., 2014). Yet considering size as an intrinsic factor is confounded by the fact that size is so closely related to average historical growth rate. This problem of cross-equation correlation is exacerbated by a generally weak ability to represent local variability in site quality as an intrinsic factor in the analytical framework. Pooling trees of varying site quality in a single analysis is likely to falsely attribute variation in growth to size instead of site quality, either because site quality is omitted or because common indicators of site quality tend to have much greater measurement error than tree size (Hember et al., 2018; Nicklen et al., 2016). Similarly, if a hypothetical improvement in growing conditions forces a sustained increase in growth, it must also translate into an equal increase in size (at a specific age). In such cases, the correlation between growth and size is at least partially spurious. Here we acknowledge that large trees are likely to have greater capacity for growth due to increasing light- and soil-harvesting capacities relative to neighbors, yet we also acknowledge that it is partially circular to consider size as a covariate of growth in pooled samples without specific measures that address correlation between size and extrinsic factors. This constitutes the first decision where potential sources of bias in both directions are recognized, but no solution is identified; leaving tree size out of multiple regression analysis may lead to overestimation (Bias 3), while including tree size may lead to underestimation of time trends in G_{sw} (Bias 4).

Conducting multiple regression analysis requires additional choices among methods of estimation (Decision 5). Common approaches include LS regression, ME models, generalized additive models, and machine learning algorithms. Although estimation methods may have variable strengths and weaknesses, we have no a priori expectation that any one of them introduces bias.

Lastly, studies face the decision of whether to account for sampling biases (Decision 6). Based on previous assessments of sampling bias (Brienen et al., 2012; Briffa & Melvin, 2011; Gloor et al., 2009; Krankina et al., 2005), we assume that failing to include such biases by defining the underlying processes as intrinsic factors in the analytical framework risks falsely attributing time trend to extrinsic forcing (Bias 5).

Estimating trends in G_{sw} indirectly from analysis of size at A_{ref} is an interesting alternative to Decision 1 because it provides a workaround to Biases 3 and 4. As with growth, we must choose among D_{ob}, BA, or B_{sw} as the dependent variables (Decision 6). As Bias 1 applies equally to size, we choose to analyze B_{sw}. For size, the general approaches to standardization (Decision 3) include analysis of cohorts (Bascietto et al., 2004; Lopatin et al., 2008), which involves choosing multiple time periods (cohorts), or multiple regression analysis (Hember et al., 2012), which involves fitting nonlinear models of stemwood biomass as functions of age and time. The models are generally fitted by selecting LS or ME as methods of estimation (Decision 4). Finally, as with growth, we assume that estimation of time trends based on analysis of size may be affected by sampling biases. As no single covariate has been identified to represent these potential effects, some type of ad hoc correction (e.g., Brienen et al., 2012) must be considered (Decision 5).

Based on the above considerations, we chose to estimate time trends in growth indirectly from analysis of tree size because analyzing size instead of growth required fewer decisions (5 versus 6) and specifically

avoided making a decision that had no clear way to avoid recognized sources of uncertainty (Biases 3 and 4). We chose to analyze stemwood biomass instead of diameter or basal area to avoid Bias 1. Emphasis was then placed on producing solutions to correct for sampling biases (Bias 5) and understanding uncertainty associated with methods of estimation, including cohort analysis and multiple regression analysis, and mixed-effect modeling.

With a rationale in place, the methods were broken down into two main steps. First, statistical models were developed to estimate time trends in the pooled tree ring sample (section 3.3). Second, simulations from an individual-tree Growth and Yield model were developed to assess the proportion of the time trend in observations that could be attributed to intrinsic forcing due to Bias 5 (section 3.4).

3.3. Estimation of Time Trends in Stemwood Biomass

Three methods of estimation were considered in the analysis of time trends in stemwood biomass. To simplify reporting, we focused on time trends in the stemwood biomass of 75-year-old trees ($A_{\text{ref}} = 75$), roughly consistent with the average age of trees from PSPs and NFI core samples (Table S1). First we estimated time trends by comparing the average size of trees of specified reference age for different time periods (Bascietto et al., 2004; Lopatin et al., 2008). Here time periods for three cohorts were defined by 10-year intervals: 1895–1904 (Cohort A), 1945–1954 (Cohort B), and 1995–2004 (Cohort C). An age-response function was fit using only the observations that occurred within the time interval of each cohort. In each case, the age response was predicted using the Chapman-Richards equation (Zeide, 1993):

$$B_{\text{sw},it} = \beta_1(1-\exp[-\beta_2 A_{it}])^{\beta_3} + \varepsilon_{it} \tag{1}$$

where $B_{\text{sw},it}$ is the stemwood biomass of tree i in year t; A is the age of tree i in year t; β_1, β_2, and β_3 are the fitted coefficients; and ε_{it} is the error. Dependence of the error on time was accounted for in the models by including first-order autocorrelation (AR1):

$$\varepsilon_{it} = AR(1) = \varphi\, \varepsilon_{it-1} + \omega_{it}, \omega_{it} \sim iid\, N\left(0, \sigma^2\right) \tag{2}$$

Time trends in growth of each variable were then indirectly inferred from differences among cohorts in the fitted estimates of B_{sw} at A_{ref}. For example, the time trend in stemwood biomass growth was inferred from the comparison of estimates of stemwood biomass of 75-year-old trees (B_{sw75}) from cohort A with that from cohort C. To verify the behavior of Bias 1, the analysis was also conducted for outside-bark diameter and basal area so that relative time trends in each variable could be compared.

The cohort analysis provides a powerful visual demonstration of time trend, yet the selection of the time intervals is arbitrary and the presence of long-term trends should distort the age response, as environmental changes would have affected younger trees over a disproportionately greater proportion of their life span (Hember et al., 2012). Regression analysis was therefore used as a more formal method of trend estimation. Having demonstrated the biases associated with use of diameter and basal area in the cohort analysis, we proceeded only to analyze time trends in stemwood biomass. The regression analysis was conducted by considering time as a covariate in the Chapman-Richards equation:

$$B_{\text{sw},it} = (\beta_1 + \beta_4 t)(1-\exp[-\beta_2 A_{it}])^{\beta_3} + \varepsilon_{it} \tag{3}$$

where t is the time and β_1, β_2, and β_3 are the fitted coefficients that define the shape of the sigmoidal relationship between size and age, and β_4 allows the overall magnitude of the age response to vary as a function of time, t. To make β_4 easy to fit and easy to interpret, t was standardized by subtracting the mean and dividing by the standard deviation (i.e., z-scored) prior to model fitting.

The time-dependent Chapman-Richards equation was first fitted using nonlinear (LS regression. It was then fitted again using ME models to include random effects at the scale of plots:

$$B_{sw,it} = (\beta_1 + b_{1i} + \beta_4 t)(1-\exp[-\beta_2 A_{it}])^{\beta_3} + \varepsilon_{it} \tag{4}$$

where the first coefficient is decomposed into fixed (β_1) and random ($b_{1,i}$) effects. During preliminary analysis, fits that considered random effects for other coefficients were not significant.

Tree ring data from Canada's NFI sample constitute incomplete data, as trees enter the sample across a wide range of establishment dates, while t_{samp} ranged from 1995 to 2010. With incomplete data, it is possible for differences in site properties to influence time trends. Any such effect should be defined as intrinsic forcing, as it does not describe effects of environmental change (Hember, Kurz, & Coops, 2017a). To test how time trends may have been affected by change in the spatial climate variability of the NFI plots (e.g., a potential shift in climate of the sample owing to additions or removals of plots to and from the sample), we expanded equation (3) to include long-term mean climate variables:

$$B_{sw,it} = (\beta_1 + \beta_4 t + \beta_5 T_i + \beta_6 W_i)(1 - \exp[-\beta_2 A_{it}])^{\beta_3} + \varepsilon_{it} \quad (5)$$

where T_i and W_i are the warm-season mean values of air temperature and soil water content over 1971–2000. Only LS estimation was considered for equation (5).

For each LS fit, we exhaustively tested the parameter space for initial coefficient estimates that led to global solutions. The best estimates from the LS fits were then used as the initial coefficient estimates in ME estimation. Results, therefore, reflect a second round of fits whereby only random effects of β_1 were included. The solutions for all models were found with R version 3.2.5 (R Core Team, 2016), using the *nlme* package.

3.4. Sampling Biases and Scaling Relationships

When measurements are confined to trees that were live at the time of sampling, the exclusion of fast-growing trees that died prior to t_{samp} may introduce positive time trend in growth and size (Brienen et al., 2012; Briffa & Melvin, 2011; Nehrbass-Ahles et al., 2014). Additional bias may arise from use of the classic sampling design (Nehrbass-Ahles et al., 2014), whereby only dominant or codominant trees are cored. As studies that calibrate Growth and Yield models consistently identify asymmetric competition among boreal forest stands (Hember & Kurz, 2018; Luo et al., 2019; Luo & Chen, 2011; Zhang et al., 2004), a proportion of any time trend in growth or size of dominant trees leading up to t_{samp} may be attributed to the gain in resources relinquished by suppressed and dying neighbors. If these potential artefacts of the sampling design are not accounted for as intrinsic forcing, the variation may be mistakenly attributed to environmental change (Bias 5 in Figure 2).

Given the scarcity of measurements for trees that died before t_{samp}, we sought instead to estimate the magnitude of the biases that occur in samples consisting of trees that were live and dominant at the time of sampling (LDS). A simple ad hoc correction was then applied to time trend estimates to avoid falsely attributing that variation to extrinsic forcing. It is assumed that, following the application of this correction, the remaining time trend was representative of net extrinsic forcing.

One established method of estimating the bias in time trends that arises from focus on LDS trees is to derive expected behavior of growth from simulations (Brienen et al., 2012). The concept behind this "model-based" approach is to simulate the population of trees within forest stands (POP) and then compare the time trend in growth of the entire population with that of a subset of trees that mimics the real-world sample (e.g., LDS trees). By driving the model with predictions of tree growth that do not vary over time, one can safely assume that any resulting time trends in the subset must be an artefact of the sampling design.

We used the model-based approach to estimate the proportion of time trend in LDS trees that could be attributed to natural dynamics by considering simulations from an individual-based model of forest biomass dynamics (section 2.3). The model was applied to 1,200 homogeneous forest stands of black spruce. As we used equations of growth, mortality, and recruitment that excluded dependence on terrain or environmental conditions (e.g., Hember et al., 2018), there was no spatial variation beyond the stochasticity of the model. Consistent with analyses by Brienen et al. (2012), the simulations were independent of calendar year, such that the predictions of individual-tree growth or biomass at any given age, $G_{sw}(A)$ and $B_{sw}(A)$, were independent of any extrinsic factors in the real world. For each stand, biomass dynamics were simulated for 1,000 years. These dimensions ensured that stochasticity in the simulations did not significantly influence results, and that tree age and stand biomass density had reached dynamic equilibrium by year 700.

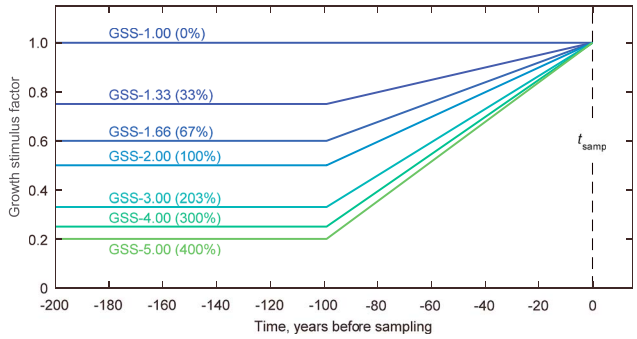

Figure 3. Growth stimulus scenarios (GSSs) used to apply varying degrees of time trend to simulations of tree growth from a Growth and Yield model. Scenarios ranged from a baseline scenario that imposed no time trend in growth (GSS-1.00) to a fivefold increase in growth (GSS-5.00) starting 100 years before the time of sampling (t_{samp}). Values in parentheses indicate the corresponding percent increase in growth.

The model of mortality was calibrated against PSP data, focusing on representing effects of ontogeny and competition. It, therefore, represented lethal processes in the high-frequency/low-magnitude part of the landscape-scale tree mortality spectrum. To account for lethal processes in the low-frequency/high-magnitude part of the landscape-scale tree mortality spectrum, stand-replacing wildfires were applied to the simulations, assuming a 100-year return interval that was constant across stands and time. Hence, in any given time step, approximately 1% of the 1,200 stands was randomly affected by stand-replacing disturbance.

From simulations, we calculated the time series of mean stemwood biomass of trees that were live and dominant at the time of sampling ($B_{sw,LDS,Model}$) and the entire population of live trees ($B_{sw,POP,Model}$). To help with interpretation of the model simulations, we additionally defined the time series of mean stemwood biomass for trees that were live at time of sampling ($B_{sw,LS,Model}$) and trees that were dominant in any time step, not just at t_{samp} ($B_{sw,D,Model}$). To be consistent with Canada's NFI sample for black spruce, we defined dominant trees as those with a value of $D_{ob,Model}$ that were within the 89th percentile ± 10% of the entire population of simulated trees in each stand. Time series of mean age of live trees (A_{POP} and $A_{,LDS}$) and mean individual-tree biomass growth ($G_{sw,POP,Model}$ and $G_{sw,LDS,Model}$) were also calculated. To understand natural dynamics at the spatial scale of stands, we also calculated mean time series of SB and SBLT.

Following from Brienen et al. (2012), the relationship between the ratio, $G_{sw,LDS,Model}/G_{sw,POP,Model}$, and time leading up to t_{samp} should represent the bias arising from selecting LDS trees. A model-based bias correction could be defined as the ratio, $r_{mb}(t) = G_{sw,LDS,Model}(t)/G_{sw,POP,Model}(t)$, and then observations could be adjusted according to $G_{sw,LDS}(t)/r_{mb}(t)$ to remove the variation explained by dynamics that are specific to LDS trees. We expanded on this in two ways. First, we tested whether the ratio in tree age, $A_{LDS,Model}/A_{POP,Model}$, also depended on time before sampling in order to dismiss the possibility that $G_{sw,LDS,Model}$ diverges from $G_{sw,POP,Model}$ in part because $A_{LDS,Model}$ diverges from $A_{POP,Model}$. Second, to gain additional clarity in the scaling relationship between POP and LDS trees, the above scenario (with no time trend imposed on growth) was designated as the baseline scenario and was supplemented by additional growth stimulus scenarios (GSSs) characterized by varying degrees of positive hypothetical time trend in growth of POP trees (Figure 3).

Whereas Hember and Kurz (2018) analyzed responses to a step change in growth, here we introduced a linear monotonic increase in growth (of all trees) over 100 years leading up to t_{samp}. When the growth stimulus factor was 1.00 (GSS-1.00), the predictions equaled that of the fitted Growth and Yield model. Hence, growth was defined by contemporary variation in growth observed at PSPs and did not vary over time steps of the simulation. This baseline scenario expressed the stand dynamics that would have occurred in the hypothetical scenario where there was no significant effect of environmental change on growth rates. Scenarios with stimulus extended to a fivefold (i.e., 400%) increase in tree growth (Figure 3).

The time-dependent Chapman-Richards equation (equation (3)) was used to predict time trends in various subsets of each GSS simulation to be consistent with the methods applied to the tree ring observations (see section 3.3). The time trend estimates derived from each of the seven GSSs were then pooled to develop scaling relationships. We focused on reporting the scaling relationship between $B_{sw75,LDS,Model}$ and three other variables of interest, including stemwood biomass of 75-year-old POP trees ($B_{sw75,POP,Model}$), stemwood biomass growth of 75-year-old POP trees ($G_{sw75,POP,Model}$), and stand biomass at 75 years after stand-replacing disturbance ($SB_{75,POP,Model}$). While $B_{sw75,POP,Model}$ and $G_{sw75,POP,Model}$ are the average value of individual 75-year-old trees (with units of kg C and kg C/year, respectively), $SB_{75,POP,Model}$ is the stand biomass density which can, in theory, deviate from $B_{sw75,POP,Model}$ depending on changes in the number of live trees. Ultimately, our objective was met by reporting the response of $G_{sw75,POP,Model}$.

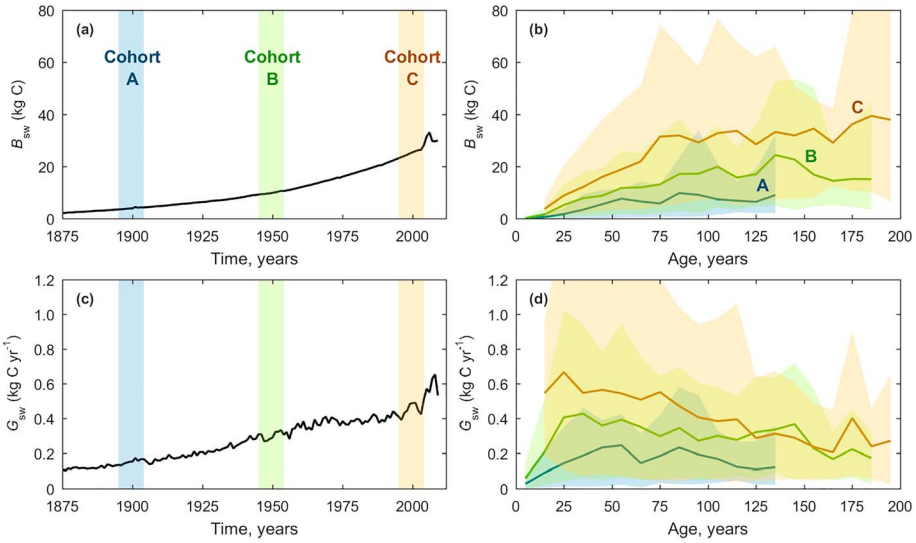

Figure 4. Relationships between individual-tree stemwood biomass (B_{sw}) and (a) time and (b) age, and relationships between individual-tree stemwood biomass growth (G_{sw}) and (c) time and (d) age. For (a) and (c), vertical bands indicate the 10-year time interval of each cohort and solid curves indicate the mean of the tree ring data for each year. In (b) and (d), solid curves and shading indicate the mean and range, respectively, in the age response of observations that occurred in the time interval of cohorts A, B, and C.

The scaling relationship between relative time trend in $B_{sw75,LDS,Model}$ and $B_{sw75,POP,Model}$ was best described by an exponential function:

$$B_{sw75,POP,Model}(t) = c_0\left(1-e^{\left[-c_1\left(B_{sw75,LDS,Model}(t)-c_2\right)\right]}\right) \quad (6)$$

where c_0 ... c_2 are the fitted coefficients and represent the maximum value of $B_{sw75,POP,Model}(t)$ the shape of the relationship and the compensation point in $B_{sw75,LDS,Model}(t)$ at which the dependent variable is equal to zero.

Uncertainty in the magnitude of the sampling bias was assumed to arise from uncertainty in process representation (i.e., the ability of the model to represent forest stand dynamics) and uncertainty in parameterization of the model. While investigating the former source of uncertainty was beyond the scope of the present study, the latter source of uncertainty was explored by conducting 200 Monte Carlo simulations. To minimize expenses, the uncertainty analysis was limited the baseline scenario, which allowed for estimation of the 95% confidence intervals in the time trend in $B_{sw75,LDS,Model}$. In total, 15 parameters varied in the simulations, including those that controlled tree growth, recruitment, and mortality (see Hember & Kurz, 2018). In each Monte Carlo simulation, new parameter sets were randomly drawn from normal distributions, as defined by a mean (best estimate) and standard deviation (2 × standard error) for each parameter.

4. Results

4.1. Cohort Analysis

Analysis of the model coefficients (Table S3) and visual inspection of the relationship between stemwood biomass and time for each cohort (Figure 4) indicated positive trends in size and growth. That is, isolating data within the time intervals of cohorts A, B, and C indicated incremental increases in size and growth across the range of tree ages recorded in the tree ring data (Figures 4b and 4d). One exception was similar growth rates of cohorts B and C for older ages (Figure 3d). It was not possible to observe trees older than 130 years in the oldest cohort (cohort A), but an age range of 25–125 remained alive at t_{samp}, for which responses can be compared among cohorts.

4.2. Regression Analysis

Coefficients of the time-dependent Chapman-Richards equations were consistently significant, including the effect of time (β_4; Table S4). Hence, for any given age of a tree, the models consistently indicated that

Table 2
Summary of Time Trends in Size of 75-Year-Old Black Spruce Trees Cored Across Canada's NFI Plots

Approach/variable	Equation	Estimation method	Sample	1901 (A)	2001 (C)	Δ (2001–1901)	Response ratio (2001/1901)
Cohort analysis:							
D_{ob}	1	LS	All sites	8.6	14.7	6.1	1.71
BA	1	LS	All sites	72.7	197.1	124.4	2.71
B_{sw}	1	LS	All sites	8.2	27.3	19.0	3.31
Regression analysis:							
B_{sw}	3	LS	All sites	6.5	27.3	20.8	4.21
B_{sw}	4	ME (FE)	All sites	20.0	29.0	9.0	1.45
B_{sw}	4	ME (RE)	All sites	14.7	22.3	7.6	1.51
B_{sw}	4	ME (FE + RE)	All sites	10.8	27.3	16.6	2.54
B_{sw}	3	LS	Upland	8.1	30.6	22.5	3.79
B_{sw}	3	LS	Peatland	6.5	19.1	12.5	2.93
B_{sw}	5	LS	All sites	7.0	27.2	20.2	3.90
B_{sw}	5	LS	Upland	11.0	30.8	19.8	2.80
B_{sw}	5	LS	Peatland	6.7	19.6	12.9	2.91

Note. Results are stratified by method (cohort analysis versus regression analysis), by indicator of size (cohort analysis only), including outside-bark diameter (D_{ob}), basal area (BA), and stemwood biomass (B_{sw}). Within regression analysis, results were conducted using least squares (LS) nonlinear regression or mixed-effect (ME) modeling. Time trends were fitted to the ME models using just the fixed effects (FE), just the random effects (RE), and both fixed and random effects (FE + RE).

stemwood biomass was significantly increasing over time. Model performance deteriorated between ME estimation with versus without random effects included in the predictions. Revising the Chapman-Richards equation to include long-term mean climate variables in addition to time did not greatly improve model performance (Table S5). Coefficients representing the effect of time remained positive and significant (Table S5).

4.3. Time Trend in the Observations

The difference between estimates of size of 75-year-old trees in cohorts C and A indicated increases with time that depended on the variable of interest. Stemwood biomass indicated the greatest response ratio of 3.31 (Table 2). Response ratios for basal area and outside-bark diameter were 2.71 and 1.71, respectively, or 82 and 52% of what the response ratio was for stemwood biomass.

Time trends derived from regression analysis varied from 4.21 for LS estimation to just 2.54 using conditional predictions from ME estimation (Table 2). Estimating time trends in the ME predictions, based on the fixed or random effects individually, indicated that both components contribute significantly to the total response ratio of 2.54 for conditional ME estimation predictions.

Stratifying the data by site type indicated a significant difference in stemwood biomass of 75-year-old black spruce trees located in peatland versus upland forest. Recognizing the distinction in site type also led to response ratios of 2.93 and 3.79 for peatland and upland sites, respectively, which were both slightly less than that for the all-data LS estimate. Considering long-term mean values of air temperature and soil water content in addition to time (using equation (5)) reduced the time trend estimate for all data from 4.21 to 3.90. Including the climate variables had no effect on the estimate of time trend for peatlands (difference between equations (3) and (5)), while it decreased the time trend estimate from 3.79 to 2.80 for uplands.

4.4. Estimation of Intrinsic Forcing

Time series of averages from the 1,200-stand landscape of the baseline scenario simulations (i.e., with no time trend imposed on growth) was summarized for various subsets of trees, including POP trees, LDS trees, trees that are dominant during any given time interval, and trees that were live at t_{samp} (Figure 5). Simulations showed similarity with the tree ring observations of tree age, stemwood biomass growth, and stemwood biomass (Figures 5b–5d). There was strong agreement in the magnitude and time trend between predicted and observed stemwood biomass growth of LDS trees (Figure 5c). Agreement was slightly weaker for age, especially in the magnitude of trend (Figure 5b), and the simulations of stemwood biomass were systematically greater than the tree ring data (Figure 5d). The coherence between simulations ($G_{sw,LDS,Model}$ and $B_{sw,LDS,Model}$) and corresponding observations derived from the tree ring sample implied that the

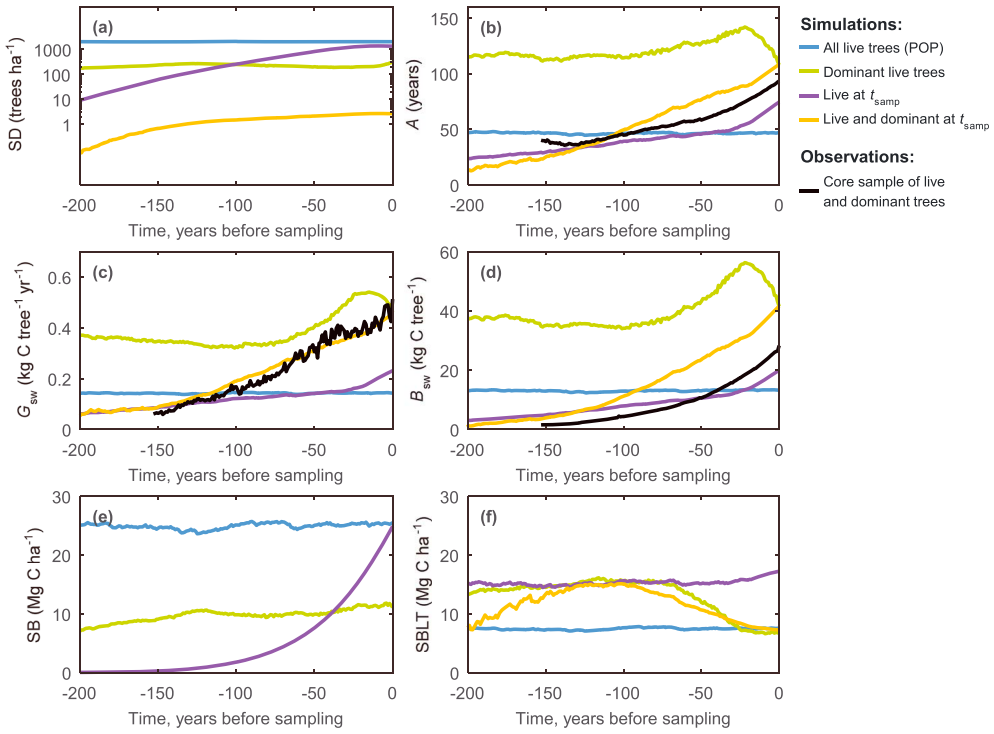

Figure 5. Baseline scenario biomass dynamics for a landscape of black spruce stands predicted by an individual-based Growth and Yield model and compared with data from tree ring chronologies. Curves indicate mean variables for 200 years leading up to the time of sampling for various subsets of trees, including all live trees considered in each time step (POP), dominant live trees in each time step, trees that were live at the time of sampling, trees that were live and dominant at the time of sampling (LDS), and observations from tree ring data. Variables include (a) stand density (SD), (b) mean age of live trees (A), (c) stemwood biomass growth (G_{sw}), (d) stemwood biomass (B_{sw}), (e) stand biomass (SB), and (f) stand biomass of larger trees (SBLT). SBLT indicates the mean competitive status of each subset.

time trend in the latter could be attributed to natural dynamics of LDS trees, as we can be certain that the baseline scenario exhibited no actual time trend. Specifically, the result is consistent with the expectation that dominant individuals benefit from outcompeting nondominant trees as they get older. However, as mean age of simulated LDS trees also increased through time, we relied on multiple regression analysis for each of the model scenarios to objectively differentiate between intrinsic and extrinsic forcings.

Applying regression analysis to simulations of stemwood biomass of trees that were live and dominant at the time of sampling, $B_{sw75,LDS,Model}$, indicated significant time trends over the last 100 years of the simulation in all growth stimulus scenarios (Figure 6a). Consistent with the significant time trend shown for LDS trees in Figure 5c, comparing $B_{sw75,LDS,Model}$ at $t_{samp} - 100$ and t_{samp} indicated a response ratio of 1.63. Assessment of the uncertainty from Monte Carlo simulations suggested 95% confidence intervals of 1.41 and 1.85. Response ratios increased from 1.63 to above 4.00 in the greatest growth stimulus scenario. Response ratios in $B_{sw75,POP,Model}$ also indicated increasing positive time trend with growth stimulus scenario, yet they started from 1.00 in the baseline scenario and only increased to 1.54 for the greatest growth stimulus scenario.

The estimates of $B_{sw75,POP,Model}$ were regressed against $B_{sw75,LDS,Model}$ to define a general scaling relationship between time trends in the two subsets (Figure 6b). Exponential functions explained almost all the variation in the relationship between LDS and POP trees across growth stimulus scenarios. As the objective of the study was to estimate time trends in growth, we developed the same scaling relationships between $B_{sw75,LDS,Model}$ and mean individual-tree growth (Figure 6c) and between $B_{sw75,LDS,Model}$ and stand growth (Figure 6d). (Stand growth is additionally affected by stand density.) From the range of time trend estimates derived from analysis of the tree ring sample, the scaling relationship suggested that the levels of growth enhancement estimated for LDS trees ought to translate into response ratios in $G_{sw75,POP,Model}$ ranging

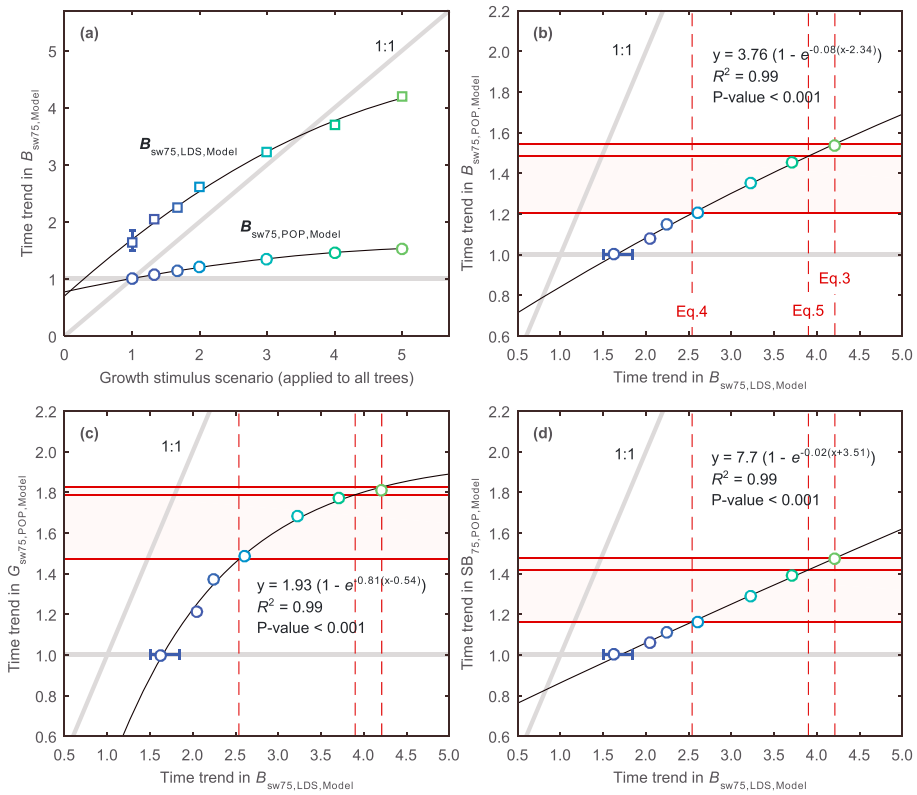

Figure 6. Scaling relationships between time trend in (a and b) stemwood biomass of 75-year-old black spruce trees that were live and dominant at the time of sampling ($B_{sw75,LDS,Model}$) and that of the entire population of trees ($B_{sw75,POP,Model}$), (c) $B_{sw75,LDS,Model}$ and stemwood biomass growth of all 75-year-old black spruce trees ($G_{sw75,POP,Model}$), and (d) $B_{sw75,LDS,Model}$ and stand biomass ($SB_{75,POP,Model}$). Results are derived from regression analysis of predictions from an individual-based Growth and Yield model calibrated against black spruce PSP data. Time trends are expressed as a response ratio: $x\,(t_{samp})/x\,(t_{samp} - 100)$. Vertical dashed red lines indicate the time trend in observations of $B_{sw75,LDS}$ from the NFI tree ring sample for black spruce using various methods of estimation (see section 3.3), while horizontal solid red lines indicate the corresponding population-level time trend estimates. Error bars indicate the 95% confidence intervals from Monte Carlo simulations conducted for the baseline scenario (Figure S4).

from 1.47 to 1.82 (Figure 6c). As expected, similar scaling relationships between time trends in $B_{sw75,LDS,Model}$ and time trends in stand biomass suggest diminished response ratios ranging from 1.16 to 1.47 (Figure 6d).

5. Discussion

5.1. Time Trends in LDS Trees

Results of the present study were based on stemwood biomass rather than diameter or basal area because variation in the latter variables is not comparable with that of stemwood biomass even when expressed as a response ratio or percent. For example, the relative time trends estimated for diameter and basal area of 75-year-old black spruce trees were 48 and 18% less than that of stemwood biomass (Table 2). As time series of tree height were not available, stemwood biomass was inferred only from ring width. The approach was, therefore, dependent on the assumption that allocation of resources to apical and cambial growth did not vary over time.

Growth trends were inferred indirectly from the dependence of stemwood biomass on time (at a specific reference age), as opposed to fitting regression models directly to growth. This avoided uncertainty in the relationship between growth and size (Sheil et al., 2017). The problem is that, under the hypothetical scenario in which extrinsic factors caused historical growth enhancement, it would also increase the size of trees at any specific age. As such, adding tree size as an independent variable in models of growth risks

underestimating extrinsic forcing, yet excluding size risks overestimating extrinsic forcing. Fortunately, the problem can be circumvented by analyzing change in stemwood biomass at a reference age.

Although cohort analysis offers an intuitive introduction to the estimation of time trends in tree growth (Figure 4 and Table 2), the potential mixing of intrinsic and extrinsic forcing is expected to distort the marginal responses of tree growth to age and size (Hember et al., 2012). As such, cohort analysis differs little from sequential standardization and seems less desirable than multiple regression analysis.

Regression analysis led to trend estimates in observed stemwood biomass of 75-year-old trees ranging from 154 to 321%, depending on whether ME or LS estimation was applied, respectively (Table 2). Both the fixed and random effects were considered in the time trend estimates from ME models because the random effects also contributed significantly to total predicted time trend. As a proportion of the among-site variation in incomplete data is consistently transferred from fixed effects, such as time, to random effects moving from LS to ME estimation, we propose that the random effects from such simplistic applications of mixed models are not necessarily random, and that the attribution of variation among growth of trees from different dates of establishment to "random" effects instead of time seems arbitrary and uninformative.

One potential explanation for positive time trends in tree growth could be the dependence between site quality and disturbance regime, as it could cause the proportions of low- and high-quality sites to vary over time (Gloor et al., 2009; Krankina et al., 2005). In boreal forests for example, old trees may be more common on poor-quality sites with lower probability of harvest and wildfire, while younger trees may be more common on high-quality sites with higher probability of harvest and wildfire. In more general terms, the use of incomplete data means that average site quality of the sample (e.g., the proportion of peatland and upland forest sites) can vary over time, or date of establishment. Even though such variation constitutes intrinsic forcing, it can be mistaken for extrinsic forcing if it is not adequately represented by the analytical framework.

When using ME estimation, a large proportion of variation in site quality must be captured by the random effects. When using LS estimation, stratifying the trend analysis by peatlands and upland forests, or including long-term mean climate as covariates in the models, did not lead to time trend estimates that strongly differed from those derived from all data (Tables 2 and S5). As such, we have greater confidence that the reported time trend was not associated with temporal variation in site quality or climate of the sample.

5.2. Intrinsic Forcing of LDS Trees

While all trend estimates suggested that B_{sw75} increased over time, reliance on the classic sampling design meant that the trend estimates were only representative of LDS trees (Brienen et al., 2012; Duchesne et al., 2019; Nehrbass-Ahles et al., 2014). Following from Brienen et al. (2012), we argued that a promising way to interpret whether time trends (from this specific sampling design) were driven by intrinsic factors was to combine the trend analysis of tree ring observations with simulations from an individual-based model of forest biomass dynamics that represents general patterns of aging, ontogeny, and competition among trees. We argued that it was beneficial to also consider multiple scenarios ranging from stationary growth to strong stimulus of growth.

A significant proportion of the time trend for LDS trees likely resulted from natural dynamics; growth of LDS trees increased with time leading up to t_{samp} even in the absence of extrinsic forcing, as indicated by the discrepancy between $B_{sw75,LDS,Model}$ and stationary growth of the population in the baseline scenario (Figure 6a). As a component of the time trend in LDS trees could be attributed to natural dynamics, our results support previous studies arguing that the classic tree ring sampling design can lead to biased estimates of the net extrinsic forcing on LDS trees (Brienen et al., 2012; Nehrbass-Ahles et al., 2014). Simply subtracting the time trend in the baseline scenario predictions of $B_{sw75,LDS,Model}$ (63%; Figures 6a and 6b) from the time trend in observed LDS trees (ranging from 154 to 321%; Table 2) yielded a time trend in stemwood biomass of 75-year-old LDS trees ranging from 91 to 258% depending on the method of estimation in multiple regression. Thus, failure to consider the natural tendency of LDS trees to exhibit increases in growth rate leading up to t_{samp} (Bias 5; Figure 2) would have led to overestimation of extrinsic forcing by 26 to 75%.

5.3. Scaling Between LDS and POP Trees

Analyzing the Growth and Yield model also allowed scaling relationships to be developed between LDS and POP trees. This is important, because a significant growth response of LDS trees to environmental change

may not translate into equivalent extrinsic forcing on entire forest stands in the presence of negative feedback mechanisms (Brienen et al., 2012; Bugmann & Bigler, 2011; Hember & Kurz, 2018; Nehrbass-Ahles et al., 2014). The development of scaling relationships for the time trend of LDS and POP trees using a Growth and Yield model suggested that the observed trends in LDS trees translated into increases in stemwood biomass growth of 75-year-old POP trees ($G_{sw,75,POP,Model}$) between 47 and 82% during the same period (Figure 6c). It is worth noting that variation in $G_{sw,75,POP,Model}$ may not scale with that of stand biomass. Roughly consistent with the general finding of low tree-growth elasticity of stand biomass density (Hember & Kurz, 2018), the relatively large observed trend estimates in growth of LDS trees translated into lower relative trends in stand biomass of 75-year-old stands ranging from 16 to 47% (Figure 6d). This behavior of the Growth and Yield model arises from the effect that increased growth of dominant trees imposes on rates of mortality, recruitment, and growth of suppressed trees (Hember & Kurz, 2018).

5.4. Limitations

Tree ring data from the classic sampling design provide observations of the growth of LDS trees. Such samples do not represent "forest growth," as they do not directly indicate the growth of nondominant trees, or potential change in stand density. Analysis of calibrated Growth and Yield models can partially overcome these limitations, emphasizing a synergy between tree ring data and repeated plot-level measurements that are used for calibration of models (Babst et al., 2014; Bowman et al., 2013; Metsaranta & Kurz, 2012). However, the reliance on models to reach these conclusions means that tree ring-based studies with the classic sampling design do not offer observation-based evidence of historical trends in tree growth.

Scaling relationships helped to constrain the magnitude of time trends in stand-level tree growth, yet the analysis did not consider potential direct environmental effects on rates of recruitment and mortality. That is, the method of scaling results from LDS trees to POP trees represented the expected feedback responses of mortality and recruitment to increased growth (via increased competition and accelerated ontogeny), but they did not represent potential direct responses of mortality and recruitment to environmental change. Hence, the estimate of time trend in stand-level tree growth may be overestimated or underestimated if environmental effects on recruitment and mortality collectively led to decreases or increases, respectively, in stand density. It is, therefore, important to acknowledge that integrated analysis of tree ring data (with the classic sampling design) and models does not provide a complete estimate of time trends in net ecosystem biomass production; it provides an estimate assuming no changes in recruitment and mortality. Collectively, these limitations emphasize the need for plot- and landscape-level monitoring systems that reflect both change in tree growth and change in tree populations (Bose et al., 2017; Chen & Luo, 2015; Hember et al., 2012; Hember, Kurz, & Coops, 2017a; Hogg et al., 2005; Michaelian et al., 2011; Zhang et al., 2018).

Although the calibrated Growth and Yield model provided a sound basis for estimating the magnitude of sampling biases, no attempt was made to understand the uncertainty in process representation, emphasizing the need for more investigation of the biases from a diversity of different growth and yield models, ideally in conjunction with samples that include entire tree populations for validation (Nehrbass-Ahles et al., 2014). In particular, the inability of the model to reproduce the full range in tree size (Figures S2a and S2d) and the inability of the model to reproduce the wide range of tree age across a extremes in the tree-size distribution (Figure S3) may indicate that such models fail to fully represent apparent trade-offs between growth rate and longevity of trees (Black et al., 2008; Johnson & Abrams, 2009), despite explicit representation of size-dependent mortality in the model. With greater knowledge of potential age dependence of historical growth trends, such models could begin to consider more sophisticated scenarios, for example, testing the hypothesis that old trees were less responsive to global change factors.

5.5. Comparison With Other Studies

These results are consistent with the common assumption in global carbon cycle science that environmental changes have accelerated tree growth (Arora et al., 2013; Ciais et al., 2013; King et al., 2007; Prentice et al., 2001). They are also consistent with experimental evidence suggesting that stemwood growth, on average, increases with increasing atmospheric nitrogen deposition, atmospheric CO_2 concentration, and air temperature (Idso & Idso, 1994; Kirschbaum & Lambie, 2015; LeBauer & Treseder, 2008; Norby et al., 1999; Saxe et al., 1998; Way & Oren, 2010; Wullschleger et al., 1995; Xia & Wan, 2008). Results are also

consistent with studies that report enhancement of stand-level forest biomass production in humid boreal and temperate climates (Fang et al., 2014; Hember et al., 2012; Hember, Kurz, & Coops, 2017a; Kauppi et al., 2014; Pan et al., 2011; Pretzsch et al., 2014).

Results of the present study differ from many other tree ring-based studies that report an absence of time trends in tree growth (Gedalof & Berg, 2010; Girardin et al., 2016; Graumlich, 1991; Jozsa & Powell, 1987; Peñuelas et al., 2011; Silva et al., 2010) or decreases in tree growth (Barber et al., 2000; Dietrich et al., 2016; Girardin et al., 2015; Housset et al., 2015). Notably, Girardin et al. (2016) report a 4% decrease in average annual basal area increment of black spruce over 1950–2002 based on analysis of Canada's NFI sample. Differences among estimates of time trends likely arise from consideration of different analysis periods. For example, Figure 4c shows a subtle decrease in the rate of growth enhancement between 1950 and 2002 when compared with the 1901–2001 period. Differences likely also arise from the different postprocessing decisions (Figure 2).

We have identified numerous ways in which common methods of analyzing tree ring data may lead to overestimation or underestimation of time trends in stemwood biomass growth (Figure 2). Analyzing ring width without any standardization will be shaped by the dependence of ring width on stemwood radius, resulting in a decline in ring width as tree diameter increases over time. Indeed, time trends in ring width often bear no resemblance to those of stemwood biomass growth. Other studies focus on basal area increment because it is more closely related to stemwood biomass growth. Although the statement is accurate, relative trends in basal area increment are still not expected to equal those in stemwood biomass growth (Table 2). Other studies inadvertently diminish, or perhaps even preclude, the possibility for temporal variation to be attributed to extrinsic factors by arbitrarily choosing to remove variance explained by intrinsic factors prior to estimation of time trends (Darlington & Smulders, 2001; Freckleton, 2002; García-Berthou, 2001). Sequential standardization is particularly problematic when performed at a site or tree level (e.g., Gedalof & Berg, 2010; Girardin et al., 2016; Housset et al., 2015), as the correlation between age and time is inevitably strong for individual trees, or samples drawn from an individual site with little variability in date of establishment. One might expect the bias from regional curve standardization to be lower, yet correlation among intrinsic and extrinsic factors in pooled samples still tends to be significant (e.g., Table S2). In general terms, if one wants to estimate the effect of factors A and B on factor C, and A and B are correlated, it is not objective to eliminate the variance in C explained by A, and then infer the variance in C explained by B based on the variance in the residuals of C explained by B. Other studies have included size as an explanatory factor in models of tree growth, which itself must change with time under the hypothetical scenario in which environmental change imposed significant extrinsic forcing. Lastly, many studies have adopted ME estimation methods, yet we find a tendency for correlation between the temporal variation attributed to random processes and extrinsic factors (e.g., time), which acts to reduce the variation attributed to extrinsic factors.

Strong positive time trends in growth reported in some studies may exaggerate the magnitude of growth enhancement if artefacts of the classic sampling design were not considered (e.g., Cole et al., 2009; Kint et al., 2012; Voelker et al., 2006). Studies reporting negligible or weak trends in tree growth seem to be inherently exempt from considering artefacts of the sampling design in the analytical framework. Conversely, Duchesne et al. (2019) make the assumption that all trees die at a specific maximum limit in tree size, without giving equal consideration to the possibility that growth rates were lower in the preindustrial era. These criticisms point to difficulties in adopting an analytical framework that does not underspecify the problem of untangling intrinsic and extrinsic forcings from tree ring data. Collectively, these potential sources of bias cast doubt on previous findings of weak or absent net extrinsic forcing on LDS trees across boreal forests of Canada.

6. Conclusions

By considering results from a range of estimation methods, and by addressing artefacts that arise from the inability to core trees that died prior to the date of sampling, we have gained confidence that environmental change was responsible for a significant proportion of positive time trend in growth rate recorded in the rings of black spruce trees across boreal forests of Canada. These results support the common assumption in carbon cycle science that increasing reactive nitrogen, atmospheric carbon dioxide concentration, and air temperature have alleviated constraints on tree growth. Although the tree rings only inform us of trends in the

growth rate of dominant trees, the analysis of growth and yield models suggested that such trends found for dominant trees ought to translate into significant, albeit lesser, trends in average growth of the entire population of black spruce trees found within forest stands. Although estimate of time trends in growth of dominant trees is fundamental to understanding how environmental change is affecting the boreal forest biome, results should not be confused for observation-based evidence of change in stand-level forest biomass production, which is equally affected by rates of recruitment and mortality.

Acknowledgments
This research was supported by the Pacific Institute for Climate Solutions. We gratefully acknowledge access to tree ring data and metadata collected by the Canadian National Forest Inventory. We also thank Christine Simard, Julie Fradette, David Gervais, Catherine McNalty, and Thierry Varem-Sanders for the contributions made to the processing of tree ring data. We thank those involved in funding, collecting, and processing of permanent sample plots, including British Columbia Ministry of Forests, Lands and Natural Resource Operations, Alberta Sustainable Resource Development, Saskatchewan Ministry of Environment Forest Service, Manitoba Conservation Forestry Branch, Ontario Ministry of Natural Resources, Nova Scotia Department of Natural Resources, New Brunswick Natural Resources, and Newfoundland and Labrador Environment and Conservation. The authors also thank Ted Hogg, Michael Michaelian, Xiaojing Guo, and Juha Metsaranta for the comments during internal review. All tree ring data used in this study are available to the public from Canada's National Forest Inventory website (https://nfi.nfis.org/en). Finally, we thank two anonymous reviewers and the Associate Editor for their constructive comments that helped improve this manuscript.

References

Arora, V. K., Boer, G. J., Friedlingstein, P., Eby, M., Jones, C. D., Christian, J. R., et al. (2013). Carbon–concentration and carbon–climate feedbacks in CMIP5 Earth system models. *Journal of Climate*, *26*(15), 5289–5314. https://doi.org/10.1175/JCLI-D-12-00494.1

Babst, F., Bouriaud, O., Alexander, R., Trouet, V., & Frank, D. (2014). Toward consistent measurements of carbon accumulation: A multi-site assessment of biomass and basal area increment across Europe. *Dendrochronologia*, *32*(2), 153–161. https://doi.org/10.1016/j.dendro.2014.01.002

Barber, V. A., Juday, G. P., & Finney, B. P. (2000). Reduced growth of Alaskan white spruce in the twentieth century from temperature-induced drought stress. *Nature*, *405*(6787), 668–673. https://doi.org/10.1038/35015049

Bascietto, M., Scarascia-Mugnozza, G., & Cherubini, P. (2004). Tree ring from a European beech forest chronosequence are useful for detecting growth trends and carbon sequestration. *Canadian Journal of Forest Research*, *34*(2), 481–492. https://doi.org/10.1139/x03-214

Beaudoin, A., Bernier, P. Y., Guindon, L., Villemaire, P., Guo, X. J., Stinson, G., et al. (2014). Mapping attributes of Canada's forests at moderate resolution through kNN and MODIS imagery. *Canadian Journal of Forest Research*, *44*(5), 521–532. https://doi.org/10.1139/cjfr-2013-0401

Beck, P. S., Juday, G. P., Alix, C., Barber, V., Winslow, S. W., Sousa, E. E., et al. (2011). Changes in forest productivity across Alaska consistent with biome shift. *Ecology Letters*, *14*(4), 373–379. https://doi.org/10.1111/j.1461-0248.2011.01598.x

Becker, M. (1989). The role of climate on present and past vitality of silver fir forests. *Canadian Journal of Forest Research*, *19*(9), 1110–1117. https://doi.org/10.1139/x89-168

Black, B. A., Colbert, J. J., & Pederson, N. (2008). Relationships between radial growth rates and lifespan within North American tree species. *Ecoscience*, *15*(3), 349–357. https://doi.org/10.2980/15-3-3149

Bond-Lamberty, B., Rocha, A. V., Calvin, K., Holmes, B., Wang, C. K., & Goulden, M. L. (2014). Disturbance legacies and climate jointly drive tree growth and mortality in an intensively studied boreal forest. *Global Change Biology*, *20*(1), 216–227. https://doi.org/10.1111/gcb.12404

Bontemps, J.-D., & Esper, J. (2011). Statistical modelling and RCS detrending methods provide similar estimates of long-term trend in radial growth of common beech in north-eastern France. *Dendrochronologia*, *29*(2), 99–107. https://doi.org/10.1016/j.dendro.2010.09.002

Bose, A. K., Weiskittel, A., & Wagner, R. G. (2017). A three decade assessment of climate-associated changes in forest composition across the north-eastern USA. *Journal of Applied Ecology*, *54*(6), 1592–1604. https://doi.org/10.1111/1365-2664.12917

Bowman, D. M. J. S., Brienen, R. J. W., Gloor, E., Phillips, O. L., & Prior, L. D. (2013). Detecting trends in tree growth: Not so simple. *Trends in Plant Science*, *18*(1), 11–17. https://doi.org/10.1016/j.tplants.2012.08.005

Brienen, R. J. W., Gloor, E., & Zuidema, P. A. (2012). Detecting evidence for CO_2 fertilization from tree ring studies: The potential role of sampling biases. *Global Biogeochemical Cycles*, *26*, GB1025. https://doi.org/10.1029/2011GB004143

Briffa, K. R., & Melvin, T. M. (2011). A closer look at regional curve standardization of tree-ring records: Justification of the need, a warning of some pitfalls, and suggested improvements in its application. In M. K. Hughes, T. W. Swetnam, & H. F. Diaz (Eds.), *Dendroclimatology, Developments in paleoenvironmental research*, (pp. 113–145). Netherlands: Springer. https://doi.org/10.1007/978-1-4020-5725-0_5

Bugmann, H., & Bigler, C. (2011). Will the CO_2 fertilization effect in forests be offset by reduced tree longevity? *Oecologia*, *165*(2), 533–544. https://doi.org/10.1007/s00442-010-1837-4

Cao, M. K., & Woodward, F. I. (1998). Dynamic responses of terrestrial ecosystem carbon cycling to global climate change. *Nature*, *393*(6682), 249–252. https://doi.org/10.1038/30460

Chen, H. Y. H., & Luo, Y. (2015). Net aboveground biomass declines of four major forest types with forest ageing and climate change in western Canada's boreal forests. *Global Change Biology*, *21*(10), 3675–3684. https://doi.org/10.1111/gcb.12994

Chen, J., Chen, W. J., Liu, J., Cihlar, J., & Gray, S. (2000). Annual carbon balance of Canada's forests during 1895–1996. *Global Biogeochemical Cycles*, *14*(3), 839–849. https://doi.org/10.1029/1999GB001207

Ciais, P., Sabine, C., Bala, G., Bopp, L., & Brovkin, V. (2013). *Carbon and other biogeochemical cycles, in: Climate change 2013: The physical basis. Contribution of Working Group I to the Fifth Assessment Report of the Intergovernmental Panel on Climate Change*. New York, USA: Cambridge University Press.

Cole, C. T., Anderson, J. E., Lindroth, R. L., & Waller, D. M. (2009). Rising concentrations of atmospheric CO_2 have increased growth in natural stands of quaking aspen (*Populus tremuloides*). *Global Change Biology*, *16*(8), 2186–2197. https://doi.org/10.1111/j.1365-2486.2009.02103.x

Cramer, W., Bondeau, A., Woodward, F. I., Prentice, I. C., Betts, R. A., Brovkin, V., et al. (2001). Global response of terrestrial ecosystem structure and function to CO_2 and climate change: Results from six dynamic global vegetation models. *Global Change Biology*, *7*(4), 357–373. https://doi.org/10.1046/j.1365-2486.2001.00383.x

Darlington, R. B., & Smulders, T. V. (2001). Problems with residual analysis. *Animal Behaviour*, *62*(3), 599–602. https://doi.org/10.1006/anbe.2001.1806

Dietrich, R., Bell, F. W., Silva, L. C. R., Cecile, A., Horwath, W. R., & Anand, M. (2016). Climatic sensitivity, water-use efficiency, and growth decline in boreal jack pine (*Pinus banksiana*) forests in Northern Ontario. *Journal of Geophysical Research: Biogeosciences*, *121*, 2761–2774. https://doi.org/10.1002/2016JG003440

Duchesne, L., Houle, D., Ouimet, R., Caldwell, L., Gloor, M., & Brienen, R. (2019). Large apparent growth increases in boreal forests inferred from tree-rings are an artefact of sampling biases. *Scientific Reports*, *9*(1), 6832. https://doi.org/10.1038/s41598-019-43243-1

Erb, K.-H., Kastner, T., Luyssaert, S., Houghton, R. A., Kuemmerle, T., Olofsson, P., & Haberl, H. (2013). Bias in the attribution of forest carbon sinks. *Nature Climate Change*, *3*(10), 854–856. https://doi.org/10.1038/nclimate2004

Esper, J., Cook, E., Krusic, P., Peters, K., & Schweingruber, F. (2003). Tests of the RCS method for preserving low-frequency variability in long tree-ring chronologies. *Tree-Ring Research*, *59*, 81–98.

Fajardo, A., & McIntire, E. J. B. (2012). Reversal of multicentury tree growth improvements and loss of synchrony at mountain tree lines point to changes in key drivers. *Journal of Ecology*, *100*(3), 782–794. https://doi.org/10.1111/j.1365-2745.2012.01955.x

Fang, J., Kato, T., Guo, Z., Yang, Y., Hu, H., Shen, H., et al. (2014). Evidence for environmentally enhanced forest growth. *Proceedings of the National Academy of Sciences*, *111*(26), 9527–9532. https://doi.org/10.1073/pnas.1402333111

Freckleton, R. P. (2002). On the misuse of residuals in ecology: regression of residuals vs. multiple regression. *The Journal of Animal Ecology*, *71*(3), 542–545. https://doi.org/10.1046/j.1365-2656.2002.00618.x

Friedlingstein, P., Cox, P., Betts, R., Bopp, L., Von Bloh, W., Brovkin, V., et al. (2006). Climate-carbon cycle feedback analysis: Results from the (CMIP)-M-4 model intercomparison. *Journal of Climate*, *19*(14), 3337–3353. https://doi.org/10.1175/JCLI3800.1

García-Berthou, E. (2001). On the misuse of residuals in ecology: testing regression residuals vs. the analysis of covariance. *The Journal of Animal Ecology*, *70*(4), 708–711. https://doi.org/10.1046/j.1365-2656.2001.00524.x

Gedalof, Z., & Berg, A. (2010). Tree ring evidence for limited direct CO_2 fertilization of forests over the 20th century. *Global Biogeochemical Cycles*, *24*, GB3027. https://doi.org/10.1029/2009GB003699

Girardin, M. P., Bouriaud, O., Hogg, E. H., Kurz, W., Zimmermann, N. E., Metsaranta, J. M., et al. (2016). No growth stimulation of Canada's boreal forest under half-century of combined warming and CO_2 fertilization. *Proceedings of the National Academy of Sciences*, *113*(52), E8,406–E8,414. https://doi.org/10.1073/pnas.1610156113

Girardin, M. P., Hogg, E. H., Bernier, P. Y., Kurz, W. A., Guo, X. J., & Cyr, G. (2015). Negative impacts of high temperatures on growth of black spruce forests intensify with the anticipated climate warming. *Global Change Biology*, *22*(2), 627–643. https://doi.org/10.1111/gcb.13072

Gloor, M., Phillips, O., Lloyd, J., Lewis, S., Malhi, Y., Baker, T., et al. (2009). Does the disturbance hypothesis explain the biomass increase in basin-wide Amazon forest plot data? *Global Change Biology*, *15*(10), 2418–2430. https://doi.org/10.1111/j.1365-2486.2009.01891.x

Graumlich, L. (1991). Sub-alpine tree growth, climate, and increasing CO_2—An assessment of recent growth trends. *Ecology*, *72*(1), 1–11. https://doi.org/10.2307/1938895

Hember, R. A., Coops, N. C., & Kurz, W. A. (2018). Statistical performance and behaviour of environmentally-sensitive composite models of lodgepole pine growth. *Forest Ecology and Management*, *408*, 157–173. https://doi.org/10.1016/j.foreco.2017.09.072

Hember, R. A., Coops, N. C., & Spittlehouse, D. L. (2017). Spatial and temporal variability of potential evaporation across North American forests. *Hydrology*, *4*(1), 5. https://doi.org/10.3390/hydrology4010005

Hember, R. A., & Kurz, W. A. (2018). Low tree-growth elasticity of forest biomass indicated by an individual-based model. *Forests*, *9*(1), 21. https://doi.org/10.3390/f9010021

Hember, R. A., Kurz, W. A., & Coops, N. C. (2017a). Increasing net ecosystem biomass production of Canada's boreal and temperate forests despite decline in dry climates. *Global Biogeochemical Cycles*, *31*, 134–158. https://doi.org/10.1002/2016GB005459

Hember, R. A., Kurz, W. A., & Coops, N. C. (2017b). Relationships between individual-tree mortality and water-balance variables indicate positive trends in water stress-induced tree mortality across North America. *Global Change Biology*, *23*(4), 1691–1710. https://doi.org/10.1111/gcb.13428

Hember, R. A., Kurz, W. A., & Metsaranta, J. M. (2015). Ideas and perspectives: use of tree-ring width as an indicator of tree growth. *Biogeosciences Discussions*, *12*(11), 8341–8352. https://doi.org/10.5194/bgd-12-8341-2015

Hember, R. A., Kurz, W. A., Metsaranta, J. M., Black, T. A., Guy, R. D., & Coops, N. C. (2012). Accelerating regrowth of temperate-maritime forests due to environmental change. *Global Change Biology*, *18*(6), 2026–2040. https://doi.org/10.1111/j.1365-2486.2012.02669.x

Hogg, E. H., Brandt, J. P., & Kochtubajda, B. (2005). Factors affecting interannual variation in growth of western Canadian aspen forests during 1951–2000. *Canadian Journal of Forest Research*, *35*(3), 610–622. https://doi.org/10.1139/x04-211

Hogg, E. H., Michaelian, M., Hook, T. I., & Undershultz, M. E. (2017). Recent climatic drying leads to age-independent growth reductions of white spruce stands in western Canada. *Global Change Biology*, *23*(12), 5297–5308. https://doi.org/10.1111/gcb.13795

Holms, R.L., 1983. Computer-assisted quality control in tree-ring dating and measurement. Tree-Ring Bull. 43.

Housset, J. M., Girardin, M. P., Baconnet, M., Carcaillet, C., & Bergeron, Y. (2015). Unexpected warming-induced growth decline in *Thuja occidentalis* at its northern limits in North America. *Journal of Biogeography*, *42*(7), 1233–1245. https://doi.org/10.1111/jbi.12508

Hunter, I., & Schuck, A. (2002). Increasing forest growth in Europe—Possible causes and implications for sustainable forest management. *Plant Biosystems*, *136*(2), 133–141. https://doi.org/10.1080/11263500212331351039

Idso, K. E., & Idso, S. B. (1994). Plant responses to atmospheric CO_2 enrichment in the face of environmental constraints: a review of the past 10 years' research. *Agricultural and Forest Meteorology*, *69*(3-4), 153–203. https://doi.org/10.1016/0168-1923(94)90025-6

Johnson, S. E., & Abrams, M. D. (2009). Age class, longevity and growth rate relationships: Protracted growth increases in old trees in the eastern United States. *Tree Physiology*, *29*(11), 1317–1328. https://doi.org/10.1093/treephys/tpp068

Jozsa, L., & Powell, J. (1987). Some climatic aspects of biomass productivity of white spruce stem wood. *Canadian Journal of Forest Research*, *17*(9), 1075–1079. https://doi.org/10.1139/x87-165

Jump, A. S., Hunt, J. M., & PeñUelas, J. (2006). Rapid climate change-related growth decline at the southern range edge of *Fagus sylvatica*. *Global Change Biology*, *12*(11), 2163–2174. https://doi.org/10.1111/j.1365-2486.2006.01250.x

Kauppi, P. E., Posch, M., & Pirinen, P. (2014). Large impacts of climatic warming on growth of boreal forests since 1960. *PLoS ONE*, *9*(11), e111340. https://doi.org/10.1371/journal.pone.0111340

King, A., Dilling, L., Zimmerman, G., Fairman, D., Houghton, R., Marland, G., et al., 2007. The First State of the Carbon Cycle report (SOCCR).

Kint, V., Aertsen, W., Campioli, M., Vansteenkiste, D., Delcloo, A., & Muys, B. (2012). Radial growth change of temperate tree species in response to altered regional climate and air quality in the period 1901–2008. *Climate Change*, *115*(2), 343–363. https://doi.org/10.1007/s10584-012-0465-x

Kirschbaum, M. U. F., & Lambie, S. M. (2015). Re-analysis of plant CO_2 responses during the exponential growth phase: Interactions with light, temperature, nutrients and water availability. *Functional Plant Biology*, *42*(10), 989–1000. https://doi.org/10.1071/FP15103

Krankina, O. N., Houghton, R. A., Harmon, M. E., Hogg, E., Butman, D., Yatskov, M., et al. (2005). Effects of climate, disturbance, and species on forest biomass across Russia. *Canadian Journal of Forest Research*, *35*(9), 2281–2293. https://doi.org/10.1139/x05-151

Lambert, M. C., Ung, C. H., & Raulier, F. (2005). Canadian national tree aboveground biomass equations. *Canadian Journal of Forest Research*, *35*(8), 1996–2018. https://doi.org/10.1139/x05-112

Lamlom, S. H., & Savidge, R. A. (2003). A reassessment of carbon content in wood: Variation within and between 41 North American species. *Biomass and Bioenergy*, *25*(4), 381–388. https://doi.org/10.1016/S0961-9534(03)00033-3

LeBauer, D. S., & Treseder, K. K. (2008). Nitrogen limitation of net primary productivity in terrestrial ecosystems is globally distributed. *Ecology*, *89*(2), 371–379. https://doi.org/10.1890/06-2057.1

Li, R., & Weiskittel, A. R. (2011). Estimating and predicting bark thickness for seven conifer species in the Acadian Region of North America using a mixed-effects modeling approach: Comparison of model forms and subsampling strategies. *European Journal of Forest Research*, *130*(2), 219–233. https://doi.org/10.1007/s10342-010-0423-y

Lopatin, E., Kolstrom, T., & Spiecker, H. (2008). Long-term trends in radial growth of Siberian spruce and Scots pine in Komi Republic (northwestern Russia). *Boreal Environment Research*, *13*, 539–552.

Luo, Y., & Chen, H. Y. H. (2011). Competition, species interaction and ageing control tree mortality in boreal forests. *Journal of Ecology*, *99*(6), 1470–1480. https://doi.org/10.1111/j.1365-2745.2011.01882.x

Luo, Y., McIntire, E. J. B., Boisvenue, C., Nikiema, P. P., & Chen, H. Y. H. (2019). Climatic change only stimulated growth for trees under weak competition in central boreal forests. *Journal of Ecology*. https://doi.org/10.1111/1365-2745.13228

Mackenzie, F. T., Ver, L. M., & Lerman, A. (2002). Century-scale nitrogen and phosphorus controls of the carbon cycle. *Chemical Geology*, *190*(1-4), 13–32. https://doi.org/10.1016/S0009-2541(02)00108-0

Martin-Benito, D., Kint, V., del Río, M., Muys, B., & Cañellas, I. (2011). Growth responses of West-Mediterranean *Pinus nigra* to climate change are modulated by competition and productivity: Past trends and future perspectives. *Forest Ecology and Management*, *262*(6), 1030–1040. https://doi.org/10.1016/j.foreco.2011.05.038

McMahon, S., Parker, G., & Miller, D. (2010). Evidence for a recent increase in forest growth. *Proceedings of the National Academy of Sciences of the United States of America*, *107*(8), 3611–3615. https://doi.org/10.1073/pnas.0912376107

Metsaranta, J. M., & Kurz, W. A. (2012). Inter-annual variability of ecosystem production in boreal jack pine forests (1975–2004) estimated from tree-ring data using CBM-CFS3. *Ecological Modelling*, *224*(1), 111–123. https://doi.org/10.1016/j.ecolmodel.2011.10.026

Michaelian, M., Hogg, E. H., Hall, R. J., & Arsenault, E. (2011). Massive mortality of aspen following severe drought along the southern edge of the Canadian boreal forest. *Global Change Biology*, *17*(6), 2084–2094. https://doi.org/10.1111/j.1365-2486.2010.02357.x

Mund, M., Kummetz, E., Hein, M., Bauer, G. A., & Schulze, E.-D. (2002). Growth and carbon stocks of a spruce forest chronosequence in central Europe. *Forest Ecology and Management*, *171*(3), 275–296. https://doi.org/10.1016/S0378-1127(01)00788-5

Nehrbass-Ahles, C., Babst, F., Klesse, S., Nötzli, M., Bouriaud, O., Neukom, R., et al. (2014). The influence of sampling design on tree-ring-based quantification of forest growth. *Global Change Biology*, *20*(9), 2867–2885. https://doi.org/10.1111/gcb.12599

Nicklen, E. F., Roland, C. A., Ruess, R. W., Schmidt, J. H., & Lloyd, A. H. (2016). Local site conditions drive climate–growth responses of *Picea mariana* and *Picea glauca* in interior Alaska. *Ecosphere*, *7*(10), e01507. https://doi.org/10.1002/ecs2.1507

Norby, R., Wullschleger, S., Gunderson, C., Johnson, D., & Ceulemans, R. (1999). Tree responses to rising CO_2 in field experiments: implications for the future forest. *Plant, Cell & Environment*, *22*(6), 683–714. https://doi.org/10.1046/j.1365-3040.1999.00391.x

Paine, C. E. T., Marthews, T. R., Vogt, D. R., Purves, D., Rees, M., Hector, A., & Turnbull, L. A. (2012). How to fit nonlinear plant growth models and calculate growth rates: an update for ecologists. *Methods in Ecology and Evolution*, *3*(2), 245–256. https://doi.org/10.1111/j.2041-210X.2011.00155.x

Pan, Y., Birdsey, R. A., Fang, J., Houghton, R., Kauppi, P. E., Kurz, W. A., et al. (2011). A large and persistent carbon sink in the world's forests. *Science*, *333*(6045), 988–993. https://doi.org/10.1126/science.1201609

Peñuelas, J., Canadell, J. G., & Ogaya, R. (2011). Increased water-use efficiency during the 20th century did not translate into enhanced tree growth. *Global Ecology and Biogeography*, *20*(4), 597–608. https://doi.org/10.1111/j.1466-8238.2010.00608.x

Peters, R. L., Groenendijk, P., Vlam, M., & Zuidema, P. A. (2015). Detecting long-term growth trends using tree rings: a critical evaluation of methods. *Global Change Biology*, *21*(5), 2040–2054. https://doi.org/10.1111/gcb.12826

Piao, S., Sitch, S., Ciais, P., Friedlingstein, P., Peylin, P., Wang, X., et al. (2013). Evaluation of terrestrial carbon cycle models for their response to climate variability and to CO_2 trends. *Global Change Biology*, *19*(7), 2117–2132. https://doi.org/10.1111/gcb.12187

Prentice, I., Farquhar, G., Fasham, M., Goulden, M., Heimann, M., Jaramillo, V., et al. (2001). *The carbon cycle and atmospheric carbon dioxide, in: Climate change 2001: The physical science basis. Contribution of Working Group I to the Fourth Assessment Report of the Intergovernmental Panel on Climate Change*. New York, USA: Cambridge University Press.

Pretzsch, H., Biber, P., Schütze, G., Uhl, E., & Rötzer, T. (2014). Forest stand growth dynamics in central Europe have accelerated since 1870. *Nature Communications*, *5*(1), 4967. https://doi.org/10.1038/ncomms5967

R Core Team (2016). *R: A language and environment for statistical computing*. Vienna, Austria: R Foundation for Statistical Computing.

Salzer, M. W., Hughes, M. K., Bunn, A. G., & Kipfmueller, K. F. (2009). Recent unprecedented tree-ring growth in bristlecone pine at the highest elevations and possible causes. *Proceedings of the National Academy of Sciences*, *106*(48), 20,348–20,353. https://doi.org/10.1073/pnas.0903029106

Saxe, H., Ellsworth, D. S., & Heath, J. (1998). Tree and forest functioning in an enriched CO_2 atmosphere. *The New Phytologist*, *139*(3), 395–436. https://doi.org/10.1046/j.1469-8137.1998.00221.x

Schofield, M. R., Barker, R. J., Gelman, A., Cook, E. R., & Briffa, K. R. (2016). A model-based approach to climate reconstruction using tree-ring data. *Journal of the American Statistical Association*, *111*(513), 93–106. https://doi.org/10.1080/01621459.2015.1110524

Sheil, D., Eastaugh, C. S., Vlam, M., Zuidema, P. A., Groenendijk, P., van der Sleen, P., et al. (2017). Does biomass growth increase in the largest trees? Flaws, fallacies and alternative analyses. *Functional Ecology*, *31*(3), 568–581. https://doi.org/10.1111/1365-2435.12775

Silva, L. C. R., Anand, M., & Leithead, M. D. (2010). Recent widespread tree growth decline despite increasing atmospheric CO_2. *PLoS ONE*, *5*(7), e11543. https://doi.org/10.1371/journal.pone.0011543

Sitch, S., Huntingford, C., Gedney, N., Levy, P., Lomas, M., Piao, S., et al. (2008). Evaluation of the terrestrial carbon cycle, future plant geography and climate-carbon cycle feedbacks using five Dynamic Global Vegetation Models (DGVMs). *Global Change Biology*, *14*(9), 2015–2039. https://doi.org/10.1111/j.1365-2486.2008.01626.x

Spiecker, H. (1999). Overview of recent growth trends in European forests. *Water, Air, and Soil Pollution*, *116*(1/2), 33–46. https://doi.org/10.1023/A:1005205515952

Stephenson, N. L., Das, A. J., Condit, R., Russo, S. E., Baker, P. J., Beckman, N. G., et al. (2014). Rate of tree carbon accumulation increases continuously with tree size. *Nature advance online publication*, *507*(7490), 90–93. https://doi.org/10.1038/nature12914

Sullivan, P. F., Pattison, R. R., Brownlee, A. H., Cahoon, S. M. P., & Hollingsworth, T. N. (2017). Limited evidence of declining growth among moisture-limited black and white spruce in interior Alaska. *Scientific Reports*, *7*(1), 15,344. https://doi.org/10.1038/s41598-017-15644-7

Voelker, S. L., Muzika, R.-M., Guyette, R. P., & Stambaugh, M. C. (2006). Historical CO_2 growth enhancement declines with age in *Quercus* and *Pinus*. *Ecological Monographs*, *76*(4), 549–564. https://doi.org/10.1890/0012-9615(2006)076[0549:HCGEDW]2.0.CO;2

Wang, T., Hamann, A., Spittlehouse, D., & Aitken, S. (2006). Development of scale-free climate data for western Canada for use in resource management. *International Journal of Climatology*, *26*(3), 383–397. https://doi.org/10.1002/joc.1247

Way, D. A., & Oren, R. (2010). Differential responses to changes in growth temperature between trees from different functional groups and biomes: a review and synthesis of data. *Tree Physiology*, *30*(6), 669–688. https://doi.org/10.1093/treephys/tpq015

Willmott, C. J., Rowe, C. M., & Mintz, Y. (1985). Climatology of the terrestrial seasonal water cycle. *Journal of Climatology*, *5*(6), 589–606. https://doi.org/10.1002/joc.3370050602

Wullschleger, S. D., Post, W. M., & King, A. W. (1995). On the potential role for CO_2 fertilization effect in forests: Estimates of the biotic growth factor based on 58 controlled-exposure studies. In G. M. Woodwell & F. T. Mackenzie (Eds.), *Biotic Feedbacks in the global climatic system: Will the warming feed the warming*? (Chap. 4, pp. 85–97). Oxford: Oxford University Press.

Xia, J., & Wan, S. (2008). Global response patterns of terrestrial plant species to nitrogen addition. *The New Phytologist*, *179*(2), 428–439. https://doi.org/10.1111/j.1469-8137.2008.02488.x

Zeide, B. (1993). Analysis of growth equations. *Forest Science*, *39*(3), 594–616. https://doi.org/10.1093/forestscience/39.3.594

Zhang, L., Peng, C., & Dang, Q. (2004). Individual-tree basal area growth models for jack pine and black spruce in northern Ontario. *The Forestry Chronicle*, *80*(3), 366–374. https://doi.org/10.5558/tfc80366-3

Zhang, T., Niinemets, Ü., Sheffield, J., & Lichstein, J. W. (2018). Shifts in tree functional composition amplify the response of forest biomass to climate. *Nature*, *556*(7699), 99–102. https://doi.org/10.1038/nature26152